



LAWRENCE  
LIVERMORE  
NATIONAL  
LABORATORY

# A Mesh Relaxation Study and Other Topics

J. Yao

May 20, 2013

## **Disclaimer**

---

This document was prepared as an account of work sponsored by an agency of the United States government. Neither the United States government nor Lawrence Livermore National Security, LLC, nor any of their employees makes any warranty, expressed or implied, or assumes any legal liability or responsibility for the accuracy, completeness, or usefulness of any information, apparatus, product, or process disclosed, or represents that its use would not infringe privately owned rights. Reference herein to any specific commercial product, process, or service by trade name, trademark, manufacturer, or otherwise does not necessarily constitute or imply its endorsement, recommendation, or favoring by the United States government or Lawrence Livermore National Security, LLC. The views and opinions of authors expressed herein do not necessarily state or reflect those of the United States government or Lawrence Livermore National Security, LLC, and shall not be used for advertising or product endorsement purposes.

This work performed under the auspices of the U.S. Department of Energy by Lawrence Livermore National Laboratory under Contract DE-AC52-07NA27344.

# ***A Mesh Relaxation Study and Other Topics***

*Jin Yao, Physicist / Applied Mathematician*

*Weapons Complex and Integration -B Division  
Lawrence Livermore National Laboratory*

## ***The Line-Sweep and Equi-Distance Mesh Relaxation***

### INTRODUCTION

In an ALE simulation of material interactions, mesh relaxation is essential for the advection phase. A commonly used mesh relaxation method for a structured mesh is the equi-potential method, which is effective, robust, easy to implement, and gives smooth mesh surfaces. However an equi-potential relaxer is associated with a few undesirable features. One of the issues is the mesh surfaces are attracted to a concave boundary, to cause poor mesh quality there. In such a case time steps can be reduced so severely to halt a simulation. Besides, an equi-potential relaxer converges slowly and can be not cost efficient in the initial set up of a problem. It works best for a Cartesian mesh, but for curve-linear mesh, an equi-potential relaxer has the tendency of undesired mesh attraction.

A new mesh relaxation concept is proposed, its nature is to evenly spacing mesh surfaces by distance, so might be called an equi-distance method. Numerical tests have shown that an equi-distance relaxer provides a better mesh quality near a concave boundary compared to an equi-potential relaxer, for meshes that roughly satisfy boundary orthogonality. An equi-distance relaxation converges faster than an equi-potential relaxation, in certain cases significantly. An equi-distance relaxer works fine with a Cartesian mesh, as well as other curve-linear meshes.

With a non-concave boundary, the new relaxation works with a line-sweeping technique in each dimension, with performing one-dimensional relaxation on each mesh line, for a multidimensional problem, and allows a fast convergence with the help of successive over-relaxations. For the more difficult case in which a concave boundary exists, an effort is made to identify a point that is evenly placed between mesh surfaces in all dimensions at the same time. An exact (iterative) or an approximate solution (non-iterative) would work for separating the mesh surfaces evenly in space. The method works best with boundary orthogonality.

The new methods are shown to improve mesh quality over equi-potential relaxations with various boundary geometries. Both its 2D and 3D version have been parallelized with ALE3D and ready to update. All the smoke-test problems tested are with successes.

# ISSUES WITH AN EQUI-POTENTIAL RELAXER

## A). Slowness of Convergence

Starting from the well known Kershaw mesh (fig 1A), an equi-potential mesh relaxer will have the mesh eventually relaxed to an equal-distance between mesh lines, with a great many iterations (fig. 1B, 1C, 1D).

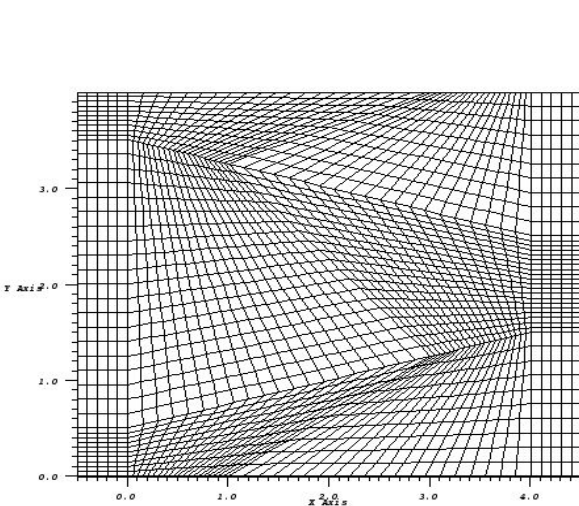


**Figure 1A. The Kershaw Mesh**

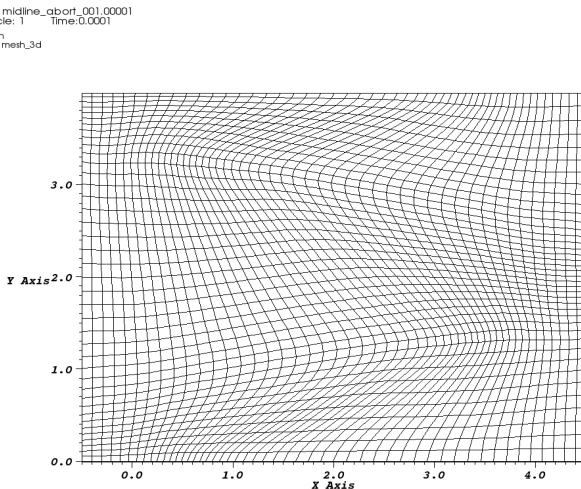


**Figure 1B. With 100 iterations using an equi-potential relaxation**

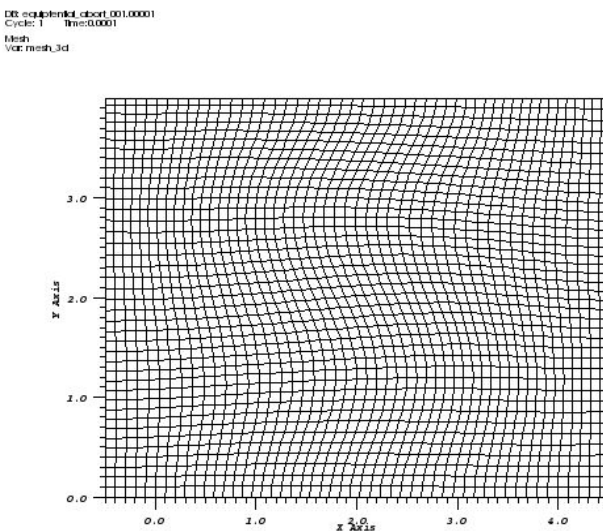


**Figure 1C. With 400 iterations.**

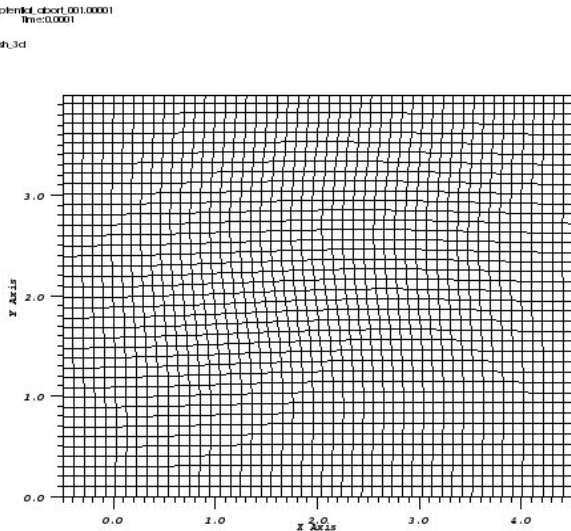


**Figure 1D. After 1000 iterations**

### *B. Mesh Attraction To Concave Boundary*

As the solution of a with an elliptic problem, equi-potential mesh lines naturally are attracted to a concave boundary (Figure 2).

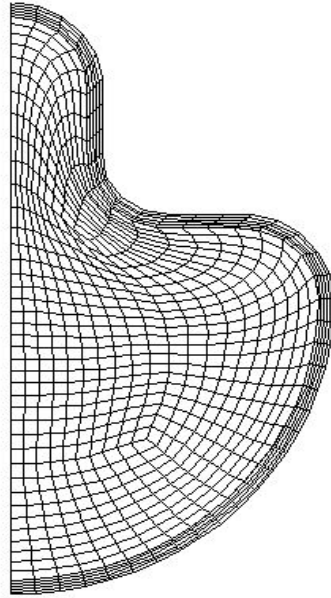


Figure 2. Mesh Attraction to a Concave Boundary with an Equi-Potential Relaxation.

### *C. Undesirable Effect with a Curve-linear Mesh*

An equi-potential mesh relaxation finds the ideal solution for a Cartesian mesh. With a curve-linear mesh, the equi-potential relaxation does not obtain the best solution, rather destroys an ideal mesh (Figure 3A, 3B).

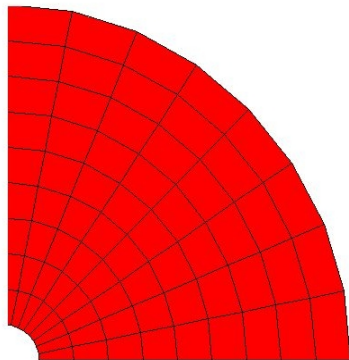


Figure 3A. Starting from an ideal mesh.

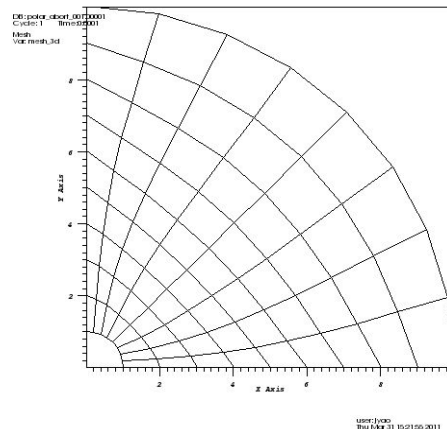


Figure 3B. After some equi-potential relaxation steps.

## THE NEW CONCEPT OF EQUI-DISTANCE

To improve mesh quality in the above cases that an equi-potential does not work ideally, the concept of equi-distance relaxation is proposed here that the mesh surfaces are to be evenly separated in space, in order to prevent undesired mesh attraction. This is demonstrated with figures 4A and 4B.

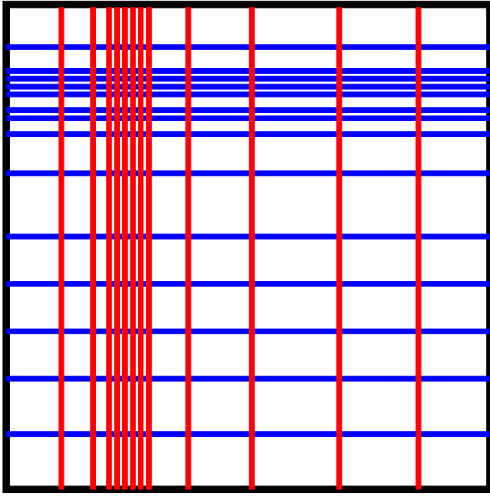


Figure 4A. A mesh with unevenly spaced mesh surfaces.

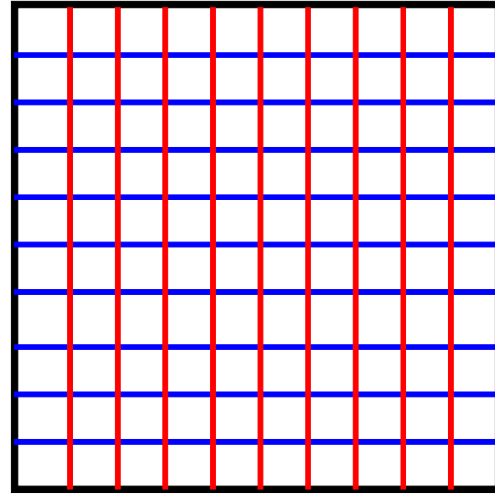


Figure 4B. Relaxed with mesh surfaces Evenly separated in space.

### *A. The Basic Stencil.*

Figure 5 shows the logical space of the basic structured stencil associated with the concept of the equi-distance relaxation. The red node is to be relaxed, blue nodes are old nodal locations

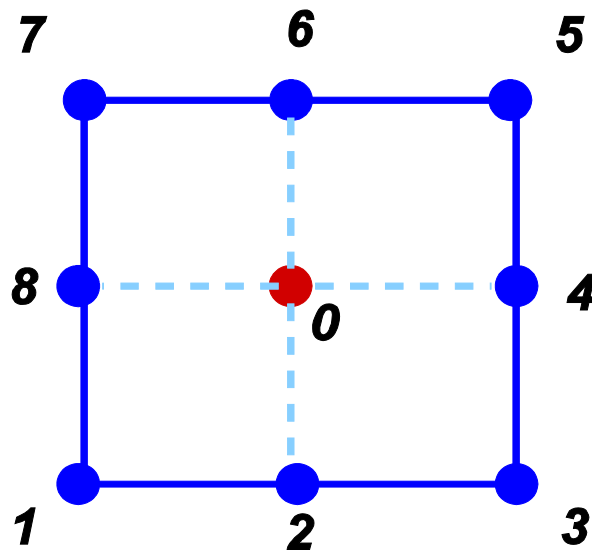


Figure 5. The basic stencil for an equi-distance relaxation.

### B. The Line-Sweeping Mesh Relaxation

With a block-structured mesh, mesh lines are well defined passing any node except, at a abnormal connectivity point. Under the condition that the boundary is non-concave, a multidimensional relaxation can be reduced to one-dimensional relaxations in each logical direction with a line-sweeping technique, demonstrated in figure 6A. One picks a mesh line with two linked segments (think it as a path to be walked on) and find the midpoint on the path (based on distance say) in the physical space. Because there are 6 paths (in 2D, 3 paths in each logical direction), one finds 6 midpoints, 3 in each logical direction that defines a new path (the broken red / green lines). The *two* broken lines can be seen as relaxed mesh lines, and their intersection (the red circle filled with yellow color) is the relaxed center node.

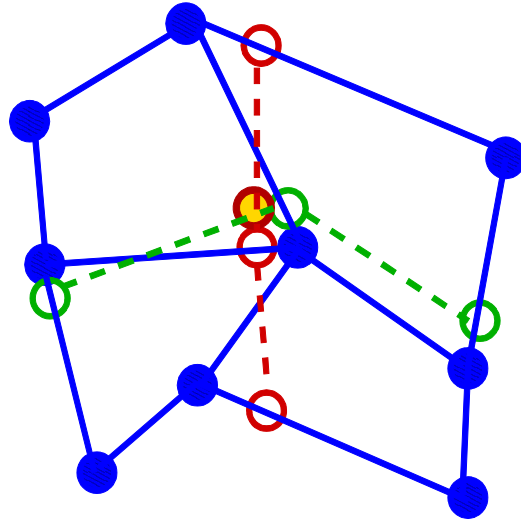


Figure 6 A. Take the intersection of two mid-lines to relax the center node.

From a global view, finding the mid-point on a path (two connected cell faces in the same logical direction) is equivalent to a one-dimensional relaxation that would eventually evenly separate nodes on a one-dimensional profile (a mesh line starting from a boundary node, ending at a boundary node, or a node at an abnormal connectivity point) according to the arc-length, see Figure 6B below.

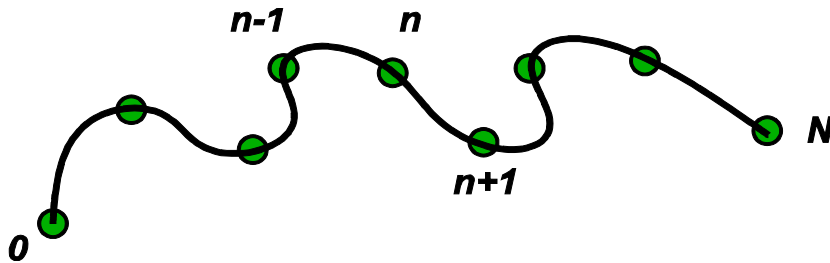


Figure 6B. Line-Sweeping by evenly separate nodes on a mesh line with arc-length.

Simply finding a mid-point is in fact the same as applying the simply averaging that

$$l_n^{new} = (l_{n-1}^{old} + l_{n+1}^{old}) / 2,$$

where  $l_n$  is the arc-length at node n. The rate of convergence can be raised by applying the successive over-relaxation (SOR), such that

$$l_n^{new} = (1 - \omega) l_n^{old} + (\omega / 2) (l_{n-1}^{old} + l_{n+1}^{old}) ,$$

With SOR the line-sweeping converges faster than the Winslow-Crowley method with the Kershaw problem, shown in figure 7 (A, B, C, D).

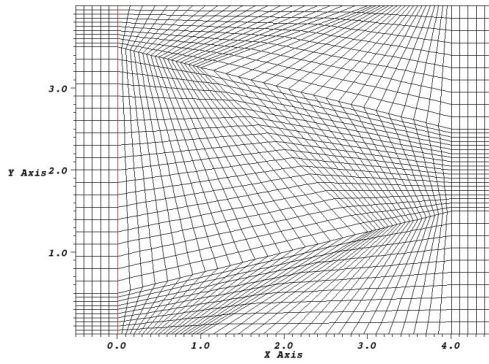


Figure 7A. The Kershaw Mesh.

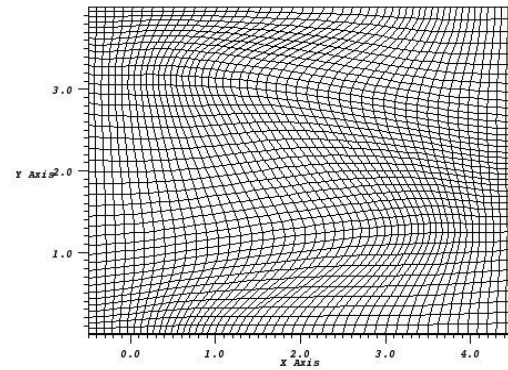


Figure 7B. Winslow-Crowley after 50 iterations.

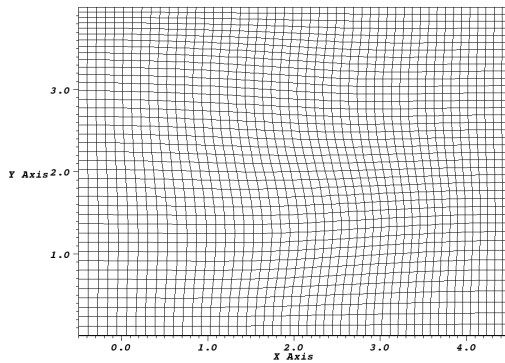


Figure 7C. Line-Sweeping with SOR after 25 iterations.

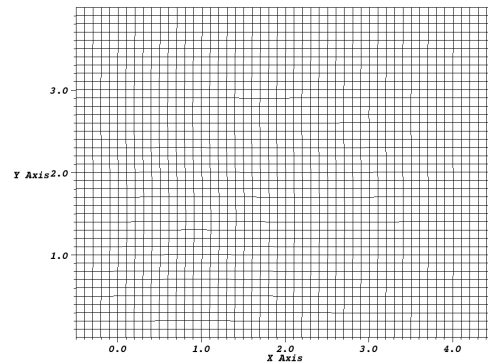


Figure 7D. Line-Sweep with SOR After 50 iterations.

### C. The Equal Distance Point

Line-Sweeping works well with problems that have non-concave boundaries. For a problem with a concave boundary, a line-sweeping method may not converge. In the other hand, evenly positioning points on a mesh line does not necessarily produce even spacing of mesh surfaces by distance, in the case that two mesh lines in different logical direction do not intersect each other with orthogonality. Therefore a more general approach is proposed, that is to find in physical space the point in the basic stencil that is equally spaced between opposing walls of the stencil. In figure 8, the equal distance point (marked by a red dot) has the same distances  $a$  and  $a$  to the top and the bottom walls of the stencil, as well as the same distances  $b$  and  $b$  to the left and the right walls.

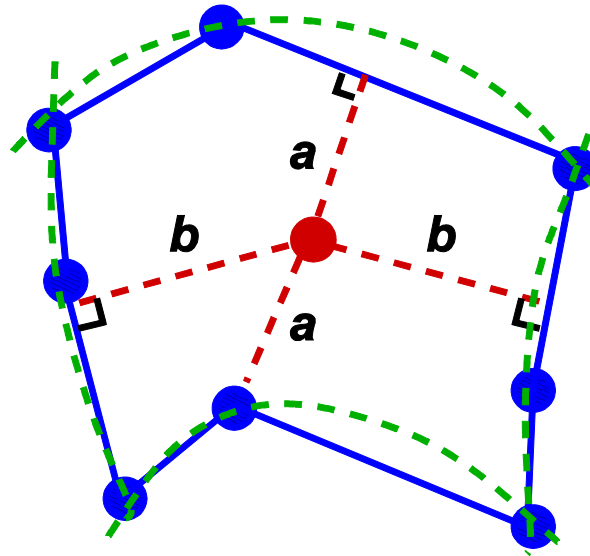


Figure 8. The equal distance point in a given stencil. The walls can be approximated with curved surfaces too (the broken green lines).

The equal-distance point is taken as the relaxed position of the center node. The equal-distance point may not be unique for a much twisted stencil in physical space but this case has not been observed in any of the numerical tests with equi-distance relaxations.

In general, the line-sweep and equal-distance point, or an equi-potential relaxation method are just different way to place the center point for a stencil. Many other possibilities to improve a block-structured mesh must exist and worth to explore.

### D. Orthogonality with Mesh Relaxation

It is evident that when mesh lines are orthogonal at a node, an effort to evenly spacing nodes on a mesh line produces evenly spaced mesh surfaces in space. This would make the line-sweep method work well. If an orthogonal solution cannot be arrived, then the orthogonality on boundary is desired to help a better performance of an equi-distance relaxer (or any other mesh relaxers).

Tangential relaxation sometimes is required to generate boundary orthogonality. Furthermore, with boundary orthogonality established by a tangential relaxation, the situation of a poor mesh quality with highly sheared elements on boundary will not occur.

### *E. Mesh Quality on A Concave Boundary*

#### *Sensitivity with boundary convexity*

An equi-potential relaxation is sensitive with boundary convexity. It tends to stretch a mesh line flat, therefore to move a node toward a concave boundary. An equi-distance relaxation tends to keep the distance the center node to boundary of the stencil, convex or concave, thus is not sensitive to boundary convexity. Figures 9A, 9B demonstrate the above said features with a basic stencil.

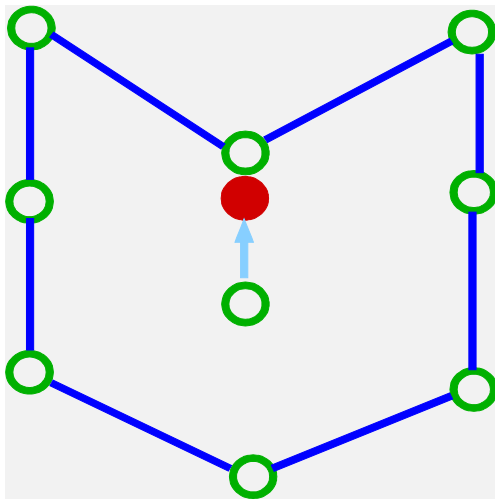


Figure 9A. An equi-potential relaxer pulls center node toward the concave boundary.

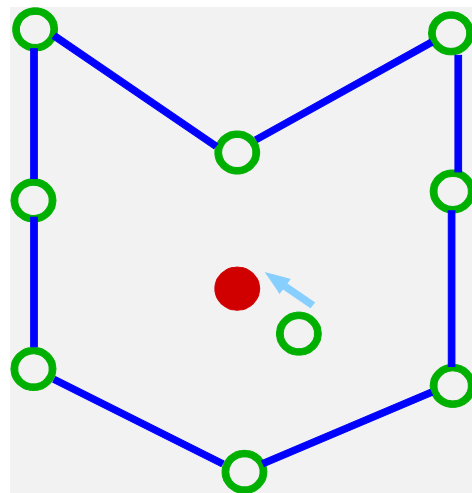


Figure 9B. An equi-distance relaxer pulls the node to center.

### *E. Mesh Symmetry with A Curve-linear Geometry*

A polar mesh (see fig. 3A) is tested with the line-sweep method, starting from a highly deformed initial mesh. After 16 iterations with SOR the mesh converges to nearly ideal (figure 10A, 10B). The natural orthogonality associated with this curve-linear mesh helps the successful application of the new equi-distance relaxation method. An equi-potential method would have attracted the radial mesh lines toward axes and the angular mesh lines toward the center.

The result shows an equi-distance relaxer keeps the geometrical symmetry well with curve-linear geometries. This is certainly an improvement compared to an equi-potential relaxer, besides the fact that an equi-distance relaxer converges faster.

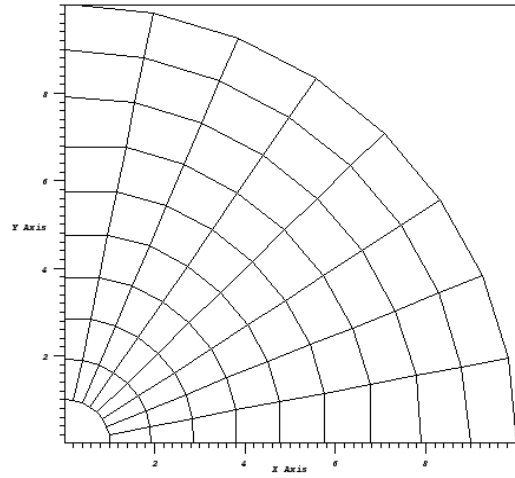
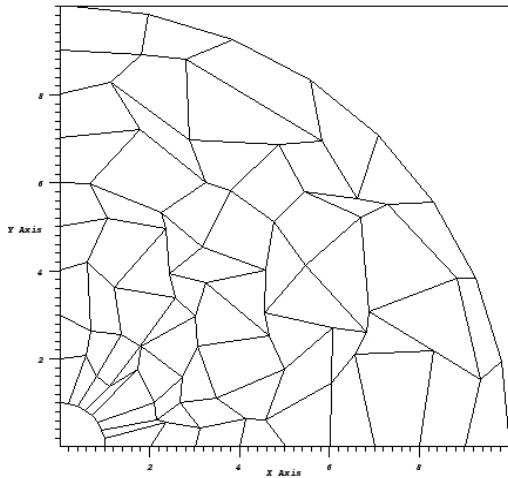


Figure 10A. A perturbed Polar Mesh.

Figure 10B. After Equi-Distance Relaxation.

### G. Treatment at an Reduced Connectivity Point

At a node where mesh lines meet abnormally, a common treatment is to move the node to the geometrical center of the triangle (tetrahedron in 3D) defined by nodes that are linked to the node at the reduced connectivity point by edges. Besides simplicity of this treatment, because the geometrical center is by nature inside the triangle (or tetrahedron), the cell-faces linked to the reduced connectivity shall not produce any concave cell. Figure 11 demonstrates this treatment and figures 12A, 12B shown the treatment work well with a butterfly-mesh with a center box.

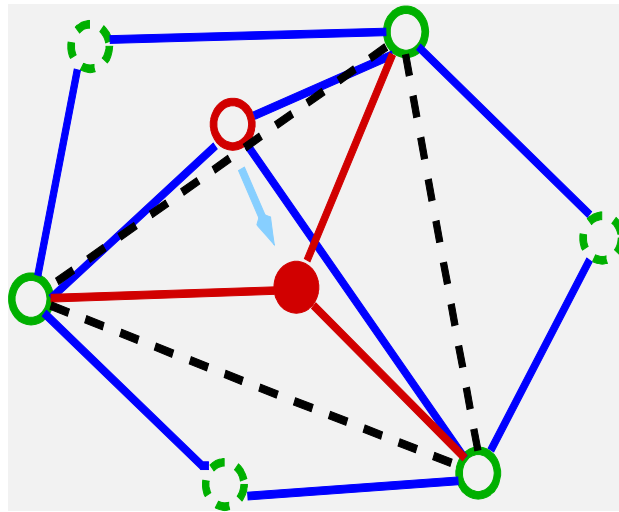
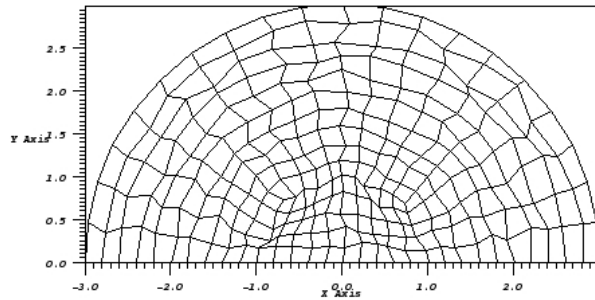


Figure 11. At a reduced connectivity point, the mesh quality is improved by moving the node in center (red circle) to the geometrical center of the triangle (broken lines) defined by the green circles.

DB: critbox\_001.00000  
 Cycle: 0 Time: 0  
 Mesh  
 Var: mesh\_3d



user: jyao  
 Wed Dec 15 14:05:53 2010

Figure 12A. A perturbed butterfly mesh.

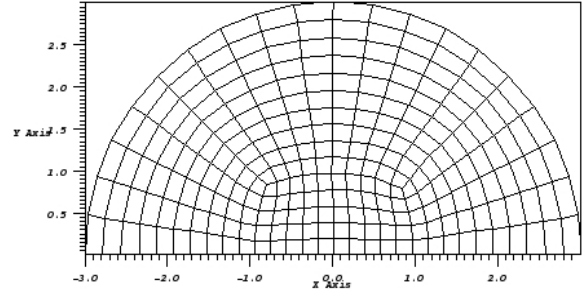


Figure 12B. Relaxed by an equi-distance.

## NUMERICAL TESTS

### *Robustness*

With an attempt to update the two-dimensional equi-distance relaxer, all the two-dimensional problems in the ALE3D smoke-test suite are run with the new relaxer with none fails. Observation of the results from test suite show well maintained symmetry, and faster convergence. See figures below.

#### 1) The smoke test BDV2D (a compression test, with the axi-symmetry)

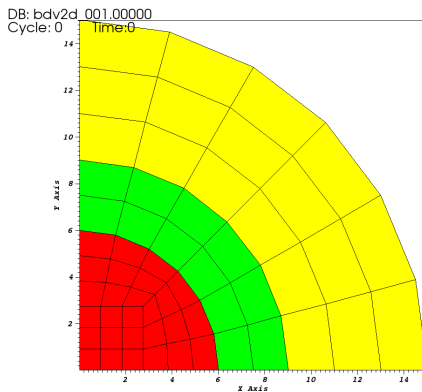


Figure 13A. the initial state

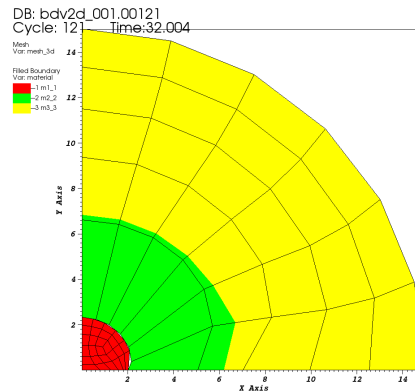


Figure 13B. Final state with equi-potential

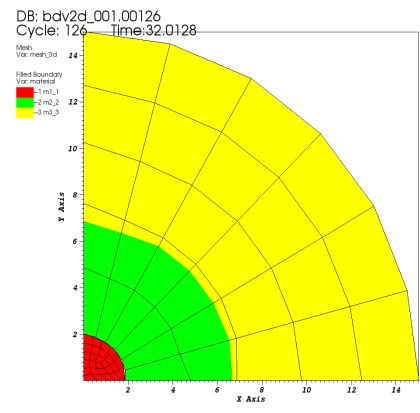


Figure 13C. Final state with equi-distance

## 2) The smoke-test ASD2D (an expansion problem, to test mesh line-spacing)

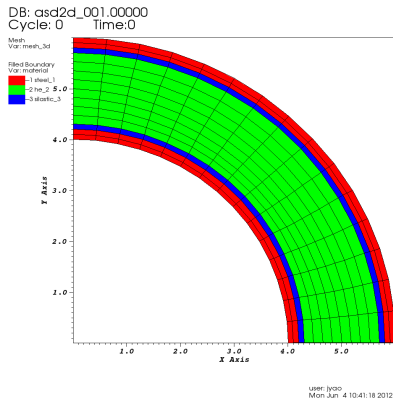


Figure 14A. Initial state

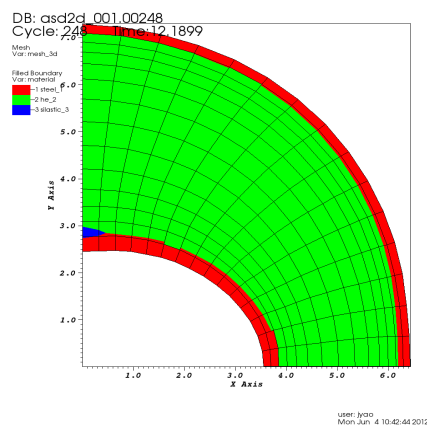


Figure 14B. Equi-potential

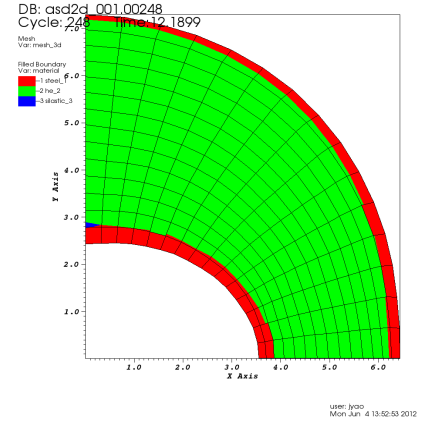


Figure 14C. Equi-distance

## 3) The smoke-test ABK2D (a simple relaxation, to test the convergence speed).

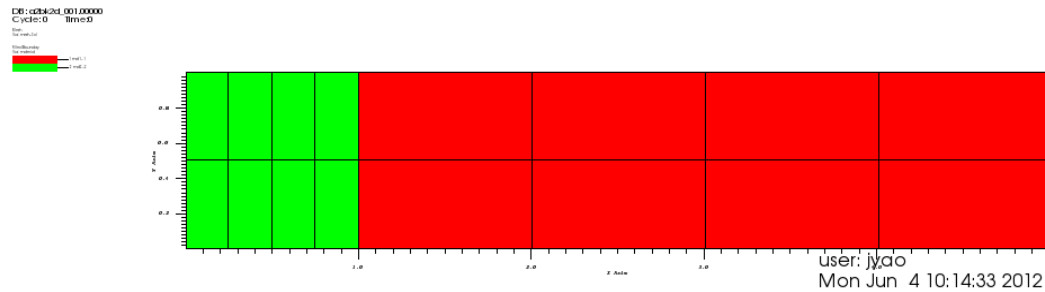


Figure 15A. The initial state.

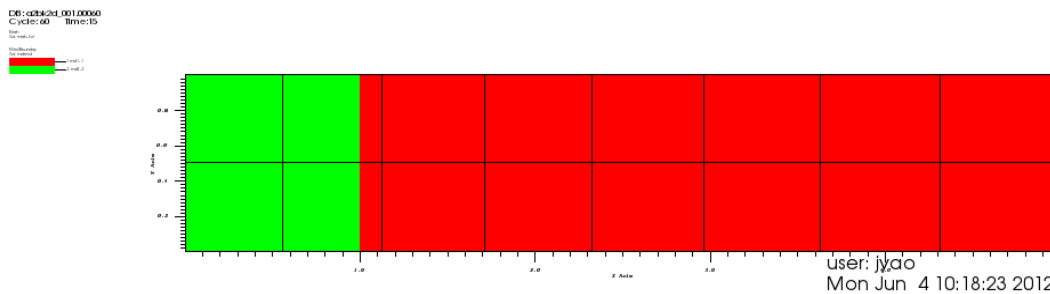


Figure 15B. Equi-potential with 20 iterations

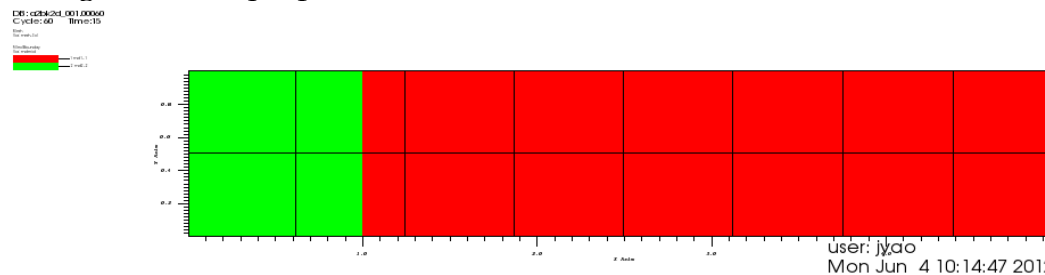


Figure 15C. Equi-distance with 20 iterations

### *Improved mesh quality on a concave boundary ( with the dented-sphere problem)*

A small tungsten ball is to impact a big steel ball filled with air and to dent the steel ball and form a concave boundary (Figures 16A, 16B).

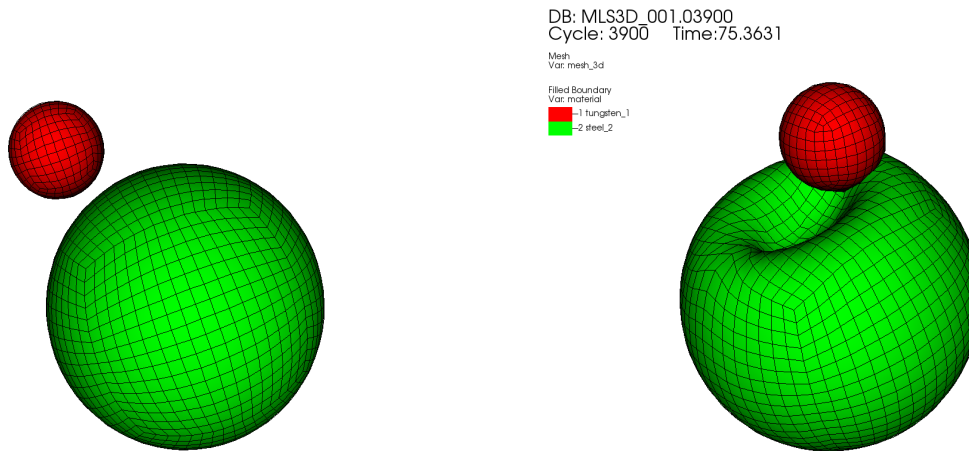
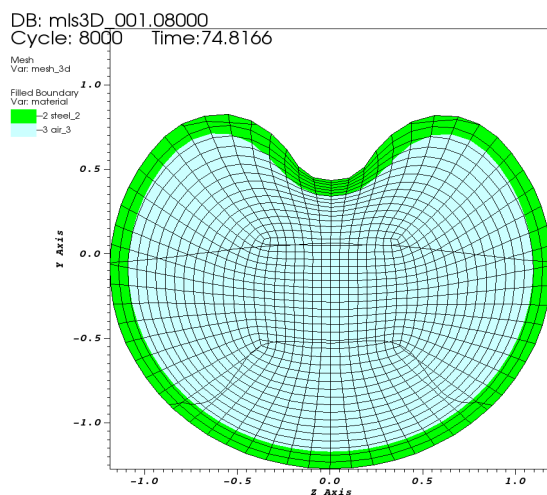


Figure 16A. A tungsten ball to impact a steel ball filled with air.

Figure 16B. After impact.

An equi-potential relaxer with ALE3D has difficulties with mesh quality near the concave boundary. The mesh surfaces squeeze into the concave boundary to form very thin cells as the dent becomes large. Very small time-steps are produced at later times as a result.

With an equi-distance relaxer implemented in ALE3D, for the same problem better separation of mesh surfaces near the concave boundary is obtained. As a result, time-steps obtained with the equi-distance relaxer is larger, which allows a smaller number of cycles.



user: jyao  
Mon Oct 8 15:59:45 2012

Fig. 17A. X cross-section, equi-potential

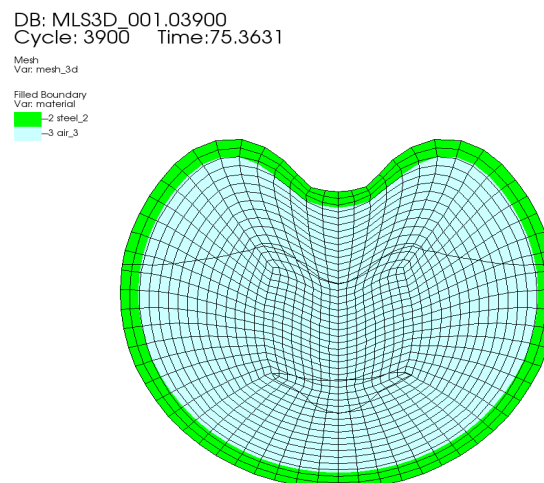
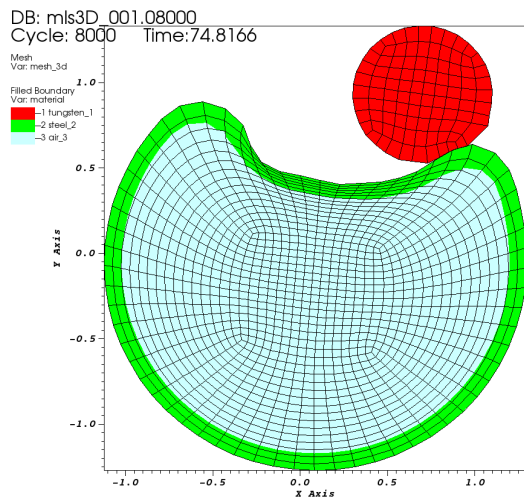


Fig. 17B. X corss-section, equi-distance

The center-box of the mesh keeps being firm with an equi-distance relaxer, this pushes the mesh surfaces toward the concave boundary to form thin cells. While the center-box of mesh with an equi-distance relaxer is crushed and this allows space for mesh surfaces for separate more for a better mesh quality (figures 17A, 17B, 17C, 17D).



user: jyao  
Mon Oct 8 16:00:00 2012

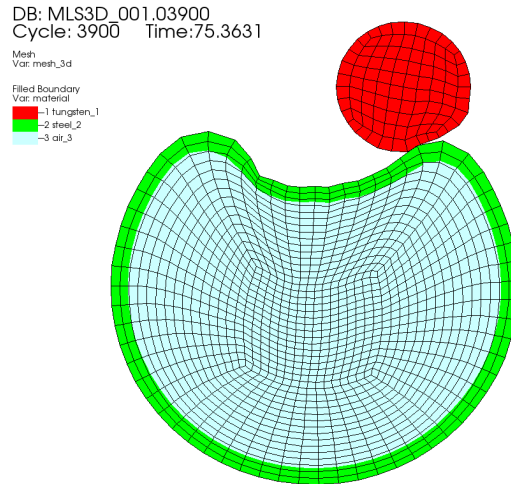
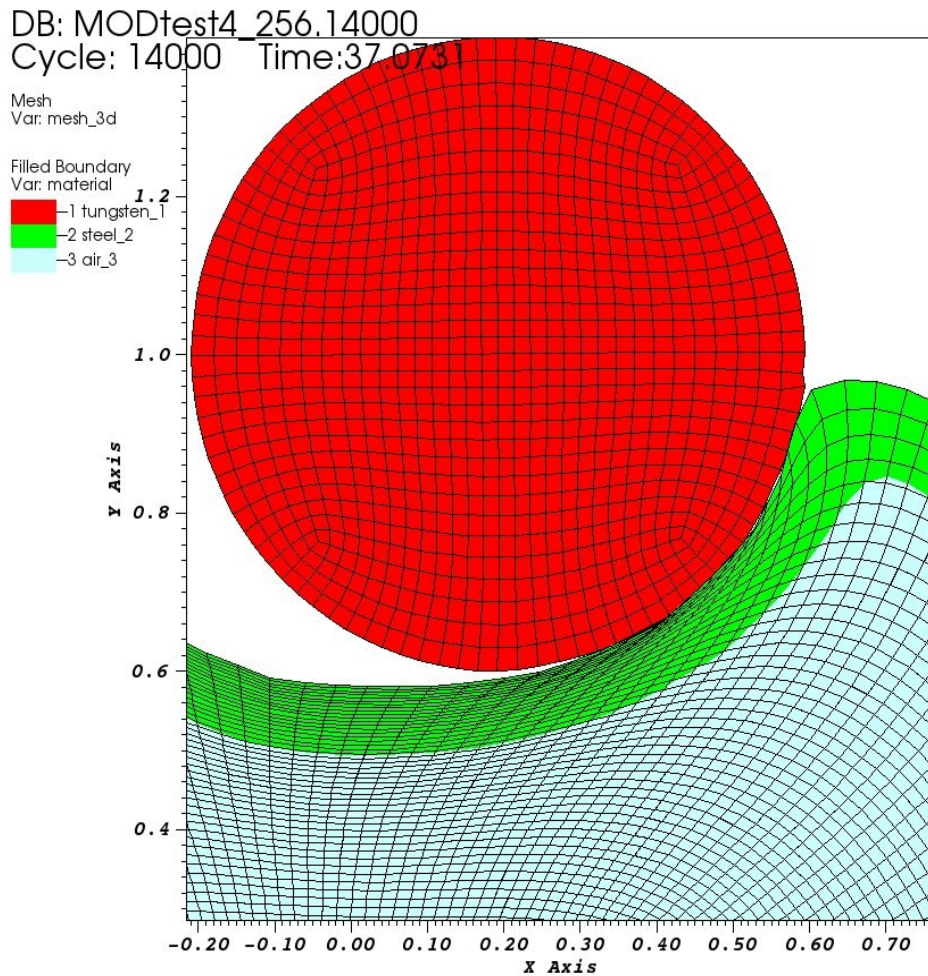


Figure 17C. Z cross-section, equi-potential      Figure 17D. Z cross-section, equi-distance

The original ALE3D methodology moves boundary nodes back to pre-relaxed positions for keeping boundary geometry, thus the concave boundary cells become highly sheared. We will show that with boundary orthogonality applied, an equi-potential gets improved mesh quality on concave boundary. Still, an equi-distance relaxer produces larger time-steps with better local mesh quality.

## PARALLELIZATION OF THE EQUI-DISTANCE RELAXATION

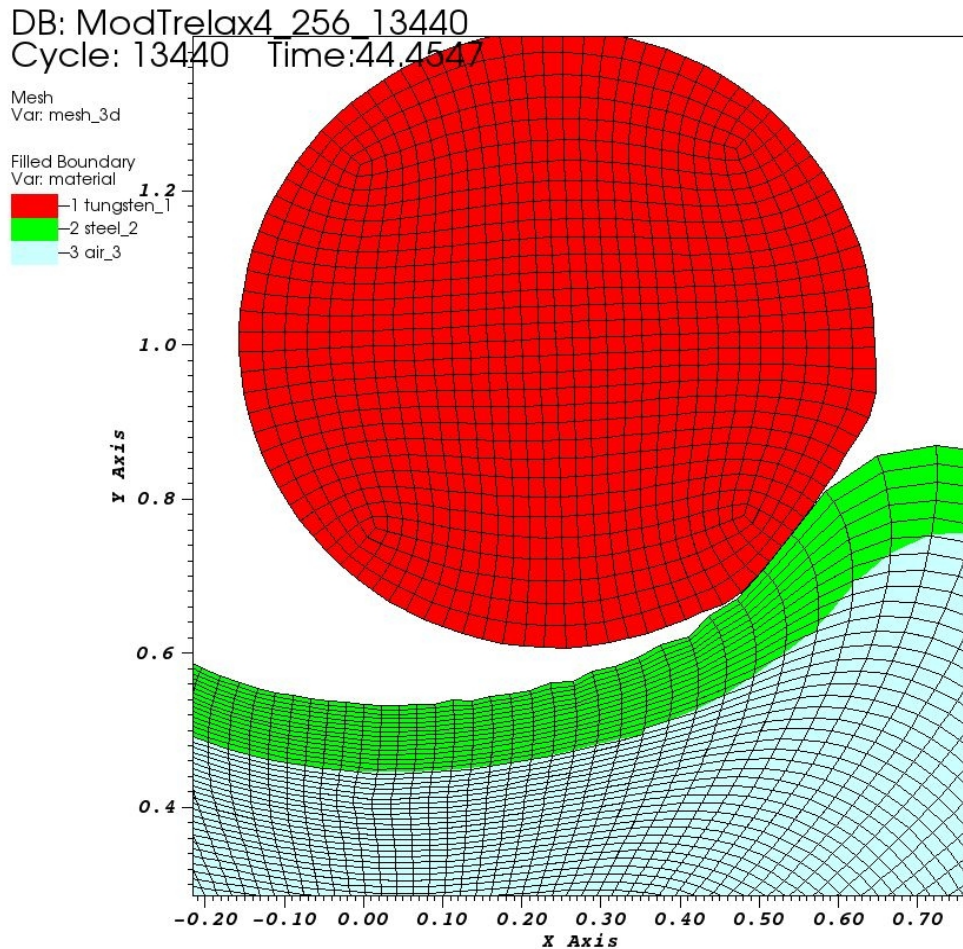
The equi-distance relaxation, with it both 2D and 3D versions, is parallelized with ALE3D. Up to 256 domain runs show consistent improvement over the default equi-potential relaxer in ALE3D regarding mesh quality near the concave boundary in the dented-sphere problem. A conservative tangential relaxation is applied sparsely in time to maintain a rough boundary orthogonality for getting rid of highly sheared zones. Without the application of the tangential relaxation, the equi-potential runs get halted in relatively early times because of poor mesh quality near the concave boundary (figure 18A). With the tangential relaxation applied sparsely, the mesh quality near the concave boundary improves and the run halted at a later time (figure 18B). With the equi-distance relaxation, a better mesh quality is obtained and with fewer cycles, the calculation went much further (figure 18C). In the case of a much denser mesh run, near vacuum region is seen to form under the concave boundary as a result of air moving from boundary in to the center. Because sound speed is up, the time step can become small. Nevertheless, with the equi-distance relaxer, better mesh quality is obtained and time steps obtained are much larger than the equi-potential relaxer.



user: jyao  
Mon Jan 14 10:12:30 2013

Figure 18A. A 256 processor run of the dented sphere problem with the default modified equi-potential relaxation, with boundary nodes unmoved.

The default relaxer generates cells with bad aspect ratio near a concave boundary, and this causes the run to halt at early time with the time step being too small.

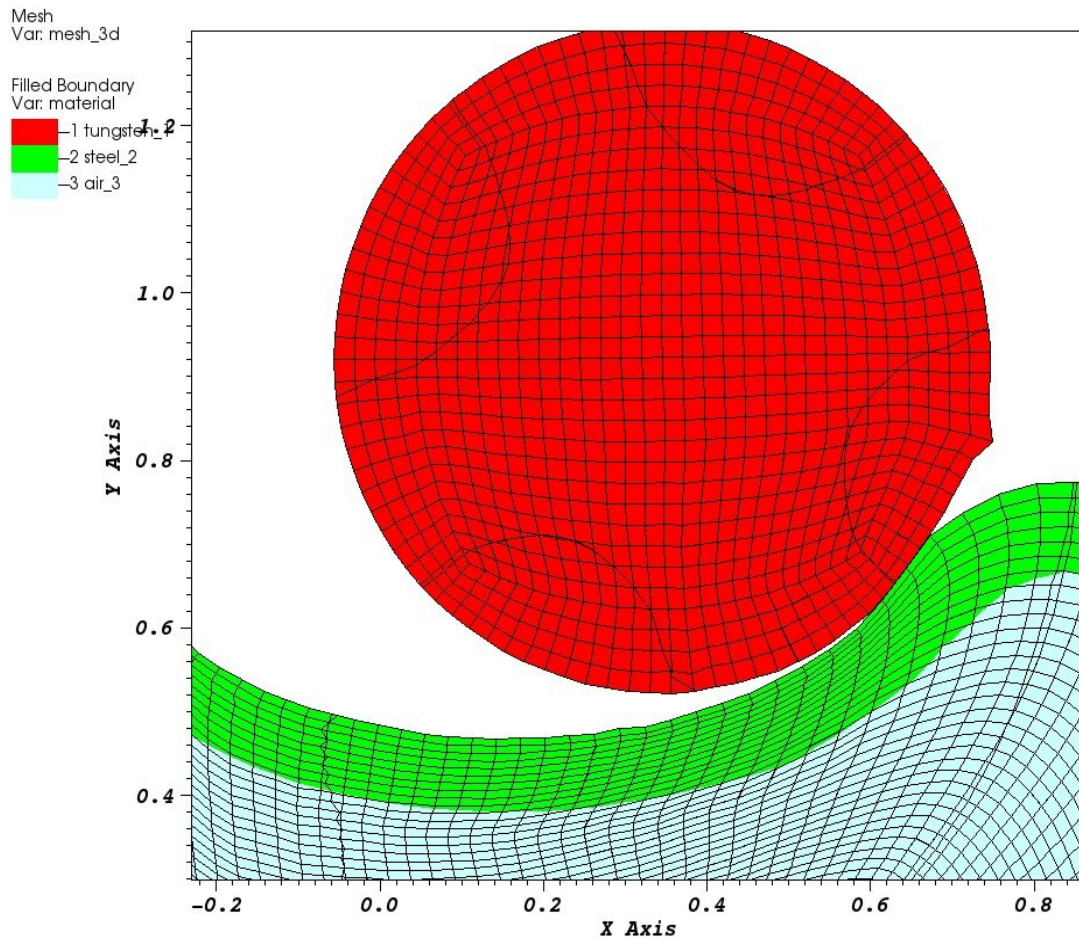


user: jyao  
Mon Jan 14 10:13:40 2013

Figure 18B. A 256 processor run of the dented sphere problem with the default modified equi-potential relaxation, with boundary orthogonality.

With a conservative tangential relaxer applied, the behavior of the default relaxer get improved with boundary orthogonality and it allows the run to go further, still very small time steps are generated and the run is nearly halted at a later time.

DB: FullTest4\_256.10000  
Cycle: 10000 Time:57.9771



user: jyao  
Mon Jan 14 10:12:12 2013

Figure 18A. A 256 processor ALE3D run of the dented sphere problem with an equi-distance relaxation, with boundary orthogonality roughly hold.

With a equi-distance relaxer, and conservative tangential relaxer applied, the mesh quality gets improved with boundary orthogonality and it allows larger time steps and the run keeps going.

## *The Moment Conserved Surface Relaxation*

A tangential relaxation is useful to establish boundary orthogonality thus to remove sheared boundary zones. This has been shown with figures 18A, 18B. However directly putting relaxed node on the pre-relaxed boundary shall definitely generate volume loss / gain with convex / concave boundary portions and the boundary geometry cannot be kept after number of such direct projections.

An new idea proposed here is to reconstruct the boundary that the set of boundary facets meant to present, then one starts from this reconstructed boundary, to setup a new set of boundary facets to represent it as the relaxed boundary. This can be done with a moment conserved local fitting as described below (for the two dimensions, the three-dimensional case is similar).

*Step 1. Construct a curved piece of surface for each boundary face with tangential moment conservation.*

In Figure 19, The curve with broken red curve is assumed the surface that the boundary face by the two red nodes and the two neighbor faces on surface meant to represent. The two black bars marks neighbor face center points and normal vectors. The yellow curve is reconstructed from the three faces with some constraints. The most important constraint is volume conservation. Thus we make the volume enclosed between the two black bars bounded by the linear facets and the curve to be reconstructed equal to each other. Next we would conserve the tangential moment the same way. Because we have four data points we may add two more constraints. One may have some freedom to choose these extra constraints. It is suggested to conserve the second tangential moment also to fit a quadratic, for a third order accuracy. It can be proven the normal moment is also conserved for a locally quadratic surface. Or make the slope of the reconstructed surface at the two black bars match the slope of the neighbor faces, for a fourth order accuracy. There can be other choices but the point is by applying some constraints we are able to define a piece of curved surface for each linear face (the yellow curve), with some conservation laws.

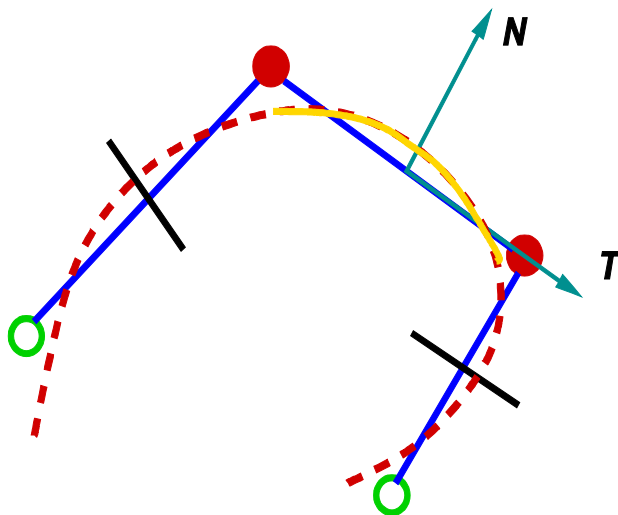


Figure 19. Reconstruct a piece of curved surface for each boundary face.

*Step 2. Reverse the previous step to construct a relaxed boundary face.*

Assemble the yellow curved facets (discontinuity be exist but because the fitting is of high order, they do not matter for the purpose setting relaxed faces), or direct fitting points on the yellow curves will produce for relaxed face a piece of curve for the relaxed face to represent (figure 20). Because each boundary node is shared by two faces, to rigorously solve the inverse construction problem requires iterations on normal nodal positions for all nodes. This may not be a mission too hard to handle because the equation at each node only involved it two neighbor nodes. Only the volume conservation is probably enough because slopes have been constrained by the reconstructed curve.

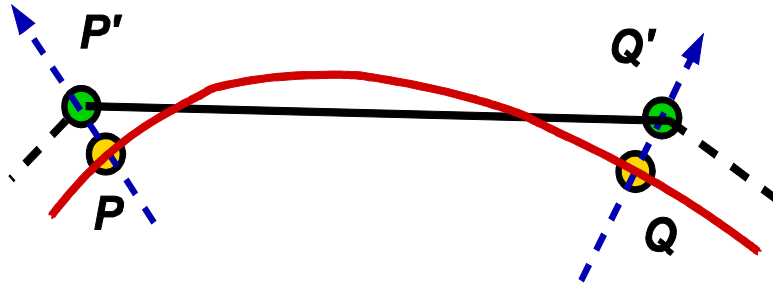


Figure 20. Inverse construction of a relaxed boundary face by moment conservation.

Another way is to lift each node ( $P$  and  $Q$  to  $P'$  and  $Q'$  in figure 20) to match volume and tangential moment bounded between that arc  $PQ$  and line-segment  $P'Q'$ . However it will cause mismatch of nodes (lifted by the left and the right faces). One has to pick a point between the two nodes to balance the volume. This operation can be repeated until convergence.

One special case is that the relaxed nodes are distributed according to a curvature law that  $\kappa A^2 = \text{const}$ , where  $\kappa$  is the curvature and  $A$  is the length of a face. In this case it can be proven that after lifting of nodes with tangential moment conservation a node has the same distance to be lifted so there will be no gaps to the leading order with this inverse construction of relaxed boundary faces. As resolution increases,  $\kappa$  varies slowly with reducing size of  $A$ , therefore equalizing boundary face length is another reasonable choice that helps conservative tangential relaxation.

### *In three-dimensions*

The three-dimensional tangential relaxation is performed by lifting and shifting boundary edges to satisfy one volume conservation, and two tangential moment conservation.

### *A lower order conservative tangential relaxation*

With the curved boundary constructed, the slope of a face to relax is kind of known. A simple way for tangential relaxation is to lift a pair of node to relax with a given slope and match volume only, looping over all faces. The solution is order dependent however give a second order solution.

### *Application of tangential relaxation with a curvature law*

A circle of radius  $0.15$  is placed at  $(0.5, 0.75)$  in a unit square domain with a velocity field  $(u, v)$  defined by

$$u = -\sin(2\pi y)\sin(\pi x)^2\cos(\pi t/8), \quad v = +\sin(2\pi x)\sin(\pi y)^2\cos(\pi t/8).$$

The circle deforms to a spiral in the velocity field above. At  $t = 4$  the spiral stretches to its maximum extend and the velocity field starts to rotate back symmetrically to time. At  $t = 8$  the original circle should be recovered. Initially the circle is presented with  $N$  points evenly distributed on the circle. The motion of these marked particles in the flow represents the change of geometry of the vortex. At integer times, the particles are redistributed in order to reduce the loss of boundary resolution with the conservative tangential relaxation described earlier in this report. The redistribution of particles are performed according to the curvature law  $\kappa a^2 = \text{const.}$  Compared to distribute points evenly along the arc-length, a distribution with the curvature law provides a more accurate representation of the spiral geometry (figures 21A, 21B, 21C).

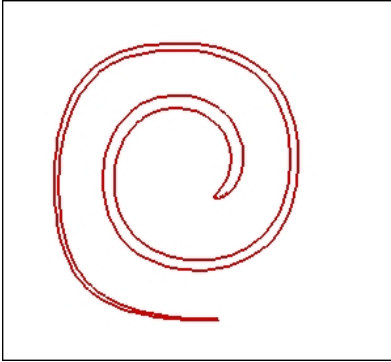


Figure 21A. Exact at  $t = 4$ .

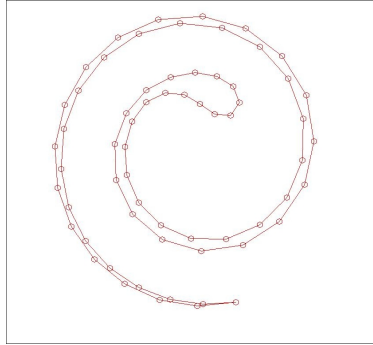


Figure 21B. 64 points distributed evenly.

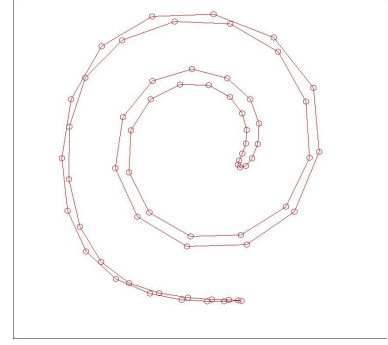


Figure 21C. 64 points distributed with  $\kappa a^2 = \text{const.}$

### *Repair a rough surface with conservative tangential relaxation*

Sometimes accumulated numerical error may generate roughness on a surface and in extreme cases a simulation can be crashed by this loss of smoothness. A conservative tangential relaxation, while maintaining conservation, can repair the roughness for a simulation to keep running. This effect can be seen in figures 22A, 22B, 22C.

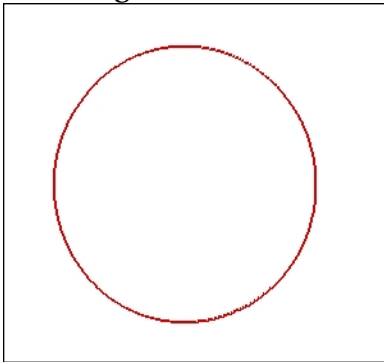


Figure 22A. Exact at  $t = 8$ .

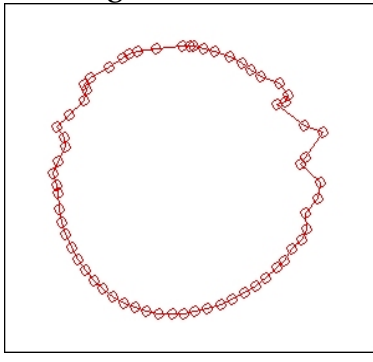


Figure 22B. Without the tangential relaxation.

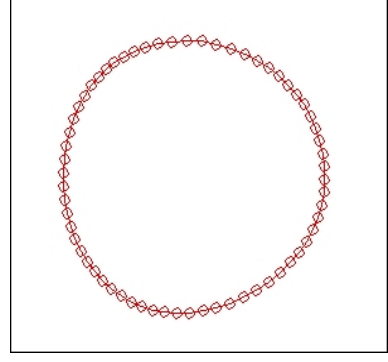


Figure 22C. With conservative tangential relaxation.

### *Parallelization of conservative tangential relaxation*

The conservative tangential relaxation in both 2D and 3D are parallelized with their lower order versions in ALE3D, and helped to obtain boundary orthogonality in parallel computations (figures 18A, 18B, 18C). Some higher order versions are coded in ALE3D, waiting for testing. Separate coding for higher order versions exist and are tested against theoretical solutions. The results show expected convergence rates.

### ***Other Related Works***

#### A GENERAL DEAD-ZONE DERIVED FROM THE DSD THEORY

An infinitely high boundary curvature on a Huygens front turning over an object (can be smooth) is shown analytically. A general dead-zone then is derived from the detonation shock dynamics (DSD). The size of the dead-zone is derived to be  $(R^2 + R_c^2)^{1/2} - R$ , where  $R$  is the local radius of curvature of the object,  $R_c$  is the detonation failure radius. This result is in agreement with the results from corner turning experiments.

#### A MARKED PARTICLE DSD FRONT TRACKER

A marked particle DSD front tracker is coded and tested against theoretical solutions for simple boundary geometries, with both the  $D_n$ - $\kappa$  relation and the DSD boundary angle condition implemented. Some numerical observations are 1). traveling DSD waves in circular (or straight) channels that do not depend on initial front geometry (fig. 23A); 2). near boundary curvature exceeds detonation failure curvature (fig. 23B, consistent with the prediction of a general dead zone).

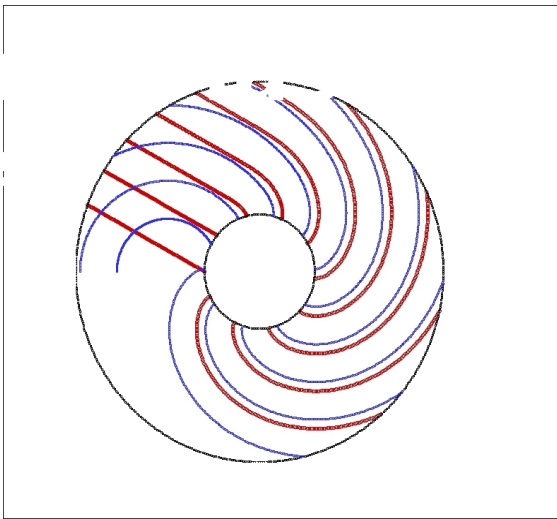


Figure 23A. Traveling wave fronts that do not depend on initial profile.

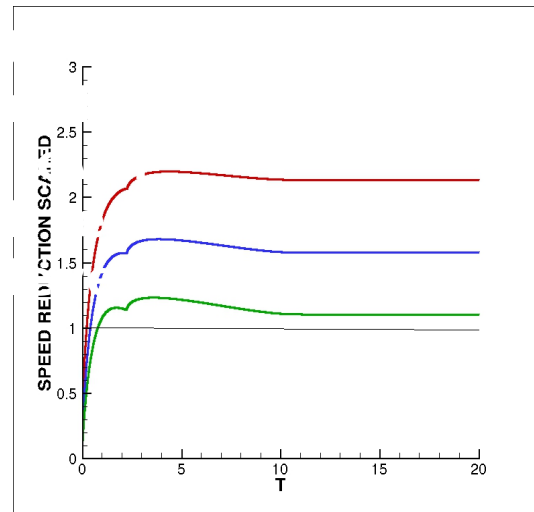


Figure 23 B. With a linear  $D_n$ - $\kappa$  relationship the terminal front curvatures exceed the failure value.

Dead zones are expected to be obtained with special  $D_n-\kappa$  curve with this marker DSD front tracker.

#### AN EFFICIENT INCLUSION TEST FOR A MASSIVE DISTRIBUTION OF POINTS

This algorithm is found with an effort to treat boundary particles with the marked particle front tracker. With a massively distributed data set and a set of closed boundary, only near boundary points are tested against local boundary geometry therefore is very efficient (fig. 24A, 24B). It should have a lot of applications for the X-scale simulations.

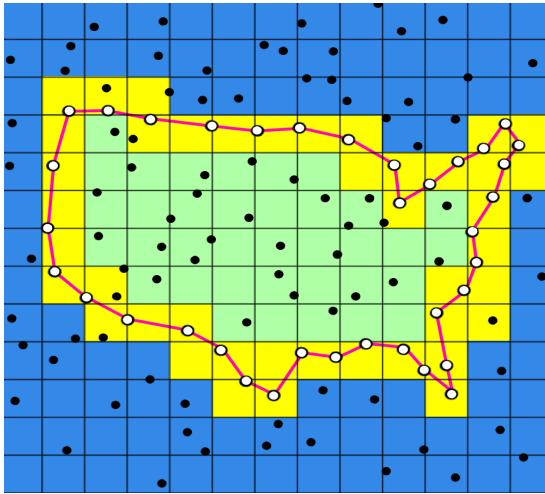


Figure 24A. Only the points contained in the yellow stripe needs to be checked.

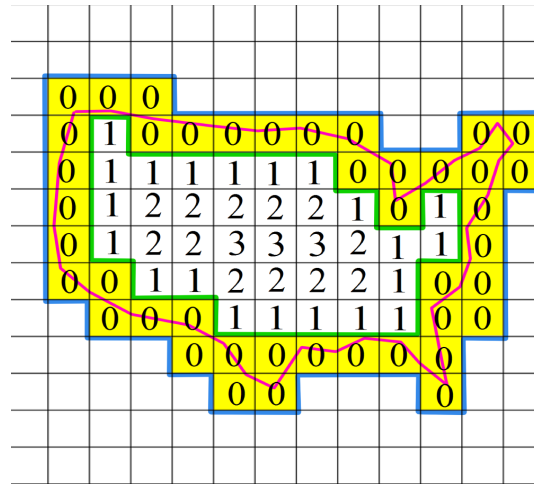


Figure 24B. Using wall-sharing relationship to find interior cubes with their logical distances to boundary.

#### A DIRECTIONAL WALKING TO REDUCE A 3D INCLUSION TEST TO 2D

A three-dimensional point inclusion problem can be reduced to an inclusion test in two dimensions with a directional walk on the three-dimensional boundary with the path of walk contained in a narrow strip of facets. By lowering the dimensionality, the cost of a higher dimensional inclusion test for a single point is reduced (Figures 25A, 25B).

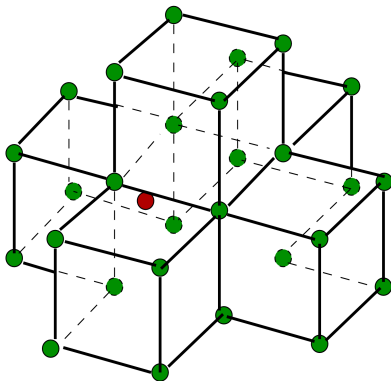


Figure 25A. A three-dimensional boundary with a point to test inclusion.

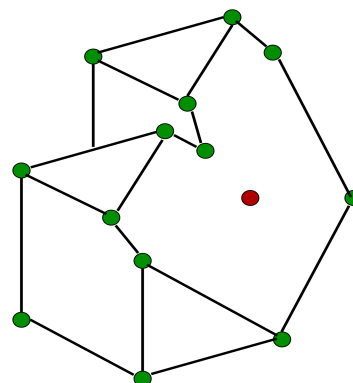
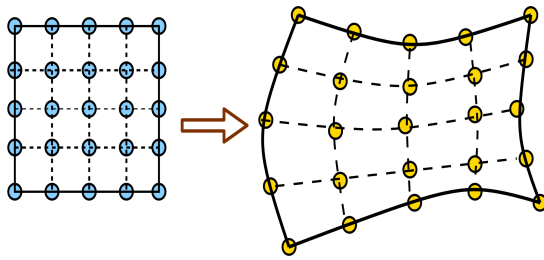


Figure 25 B. After slicing by a plane with a directional walk, it becomes a 2D problem.

The above method is efficient when the boundary is represented by a great many facets.

## TRACER PARTICLE LOCATIONS IN HIGH-ORDER OR ARBITRARY PLANAR MESHES

For a set of tracer particles distributed in a mesh with high-order elements, (or arbitrary planar cells), utilizing a background virtual cubicle complex, a distribution of pseudo nodes, or a directional walking, each non-empty cube finds a local set of elements that intersect it. For each particle contained in the cube, local inclusion tests help to find its owner cell /element (figures 26A, 26B, 26C, 26D).



*Logical Space*

*Physical Space*

Figure 26A. Mapping pseudo nodes.

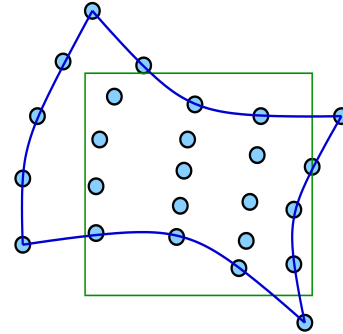


Figure 26B. Drop pseudo nodes in a virtual cube.

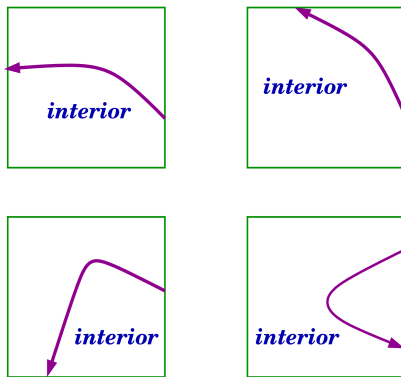


Figure 26C. Possible paths of walk in a virtual cube.

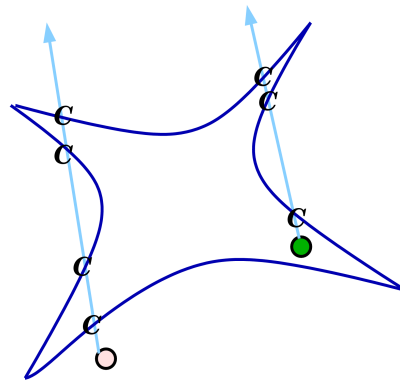


Figure 26D. Local inclusion tests.

## C-FUNCTIONS OF GENERAL INTERSECTION OF OBJECTS

A number of functions to determine intersections of various planar /curved geometries are coded in C and tested in ALE3D as needed for the mesh-relaxation study. They are useful for general purposes. Many of them are not available in ALE3D. An update of these functions would be valuable for future development of ALE3D.